

Competition of Lamellar Orientation in Thin Films of a Symmetric Poly(styrene)-*b*-poly(L-lactide) Diblock Copolymer in Melt State

Dongju Chen, Yumei Gong,[†] Haiying Huang, and Tianbai He*

State Key Laboratory of Polymer Physics and Chemistry, Changchun Institute of Applied Chemistry, Chinese Academy of Sciences, Changchun 130022, P. R. China

Fajun Zhang*

Institut für Angewandte Physik, Universität Tübingen, 72076 Tübingen, Germany

Received April 19, 2007; Revised Manuscript Received July 4, 2007

ABSTRACT: We have studied the lamellar orientation in thin films of a model diblock copolymer, symmetric poly(styrene)-*b*-poly(L-lactide) (PS-PLLA), in the melt state on supported silicon wafer surface. In this system, while the PLLA block prefers to wet the polymer/substrate interface, the polymer/air as well as polymer/polymer interface is neutral for both blocks due to the similar surface energies of PS and PLLA in melt state. Our results demonstrate that the interplay of the interfaces during phase separation results in a series of structures before approaching the equilibrium state. Lamellar orientation of thin films with different initial film thicknesses at different annealing stages has been investigated using atomic force microscopy (AFM), transmission electronic microscopy (TEM), and X-ray photoelectron spectroscopy (XPS). It is found that in the early stage (annealing time $t < 10$ min), the polymer/substrate interface dominates the structure evolution, leading to a parallel lamellar structure with holes or islands formed depending on the initial film thickness. Later on, the neutral air interface becomes important and leads to a transition of lamellar orientation from parallel to perpendicular. It is interesting to see that for films with thickness $h > 2L$, where L is the bulk lamellar period, the lamellar orientation transition can occur independently in different parallel lamellar domains due to the neutrality of polymer/polymer interface. This independent transition leads to a new intermediate stage; i.e., the perpendicular lamellae in two adjacent layers can be either parallel or cross to each other. Certainly, these interlaced structures are not the thermodynamic equilibrium forms; they emerge into the uniformed perpendicular structure upon further annealing.

Introduction

When phase separation of a diblock copolymer occurs in thin films, the effect imposed by interfaces dominate the final morphology and structure.^{1–3} In contrast to its behavior in bulk state in which the grains orient randomly with respect to each other, the microdomains formed in thin films have a preferred orientation with respect to the interface. Taking advantage of this effect and combining with other external fields, such as electric field, one can now create well-defined nanopatterns over large areas.^{4,5} This technique has been widely used nowadays in nanotechnologies.⁶

Since the past decade, there is a significant amount of research related to the orientation of symmetric block copolymer.^{1–13} For symmetric diblock copolymer, phase separation results in a lamellar structure with two alternative phases. In thin films on supported substrate, specific interactions between polymer, air, and substrate determine the final lamellar orientation. If two blocks have different surface energies, the block with lower surface energy wets the air interface and the block with a preferential interaction to the substrate wets the substrate. There are two types of lamellar structures:^{2,3,7–9} (a) symmetric structure if the same block segregates to both interfaces and (b) antisymmetric structure if each interface absorbs different

components. In both cases, the lamellar structure is parallel to the substrate. The film thickness (h) is quantized as $h = nL$ for symmetric system or $h = (n + 1/2)L$ for antisymmetric system, where L is the bulk value of the copolymer lamellar period and n is an integer. If the initial film thickness is not commensurate with these values, relief structures of islands or holes with a step height of L form on the surface of the thin films.

If the substrate is neutral for both blocks in symmetric diblock copolymer, a perpendicular lamellar structure could be formed near the substrate. A hybrid structure with parallel and perpendicular lamellar mixture could be formed from air surface and neutral substrate. Recently, the formation of perpendicular lamellae in symmetric diblock copolymer thin film has been reported in theory^{14,15} and experiment.^{16–27} Self-consistent mean-field theory predicts that perpendicular orientation is more favorable at a neutral interface due to higher conformational freedom.¹⁴ Sivaniah et al. have investigated the effect of the roughness of the substrate on the structure of the symmetric PS-PMMA diblock copolymer thin film.^{20,21} They found that the roughness of a substrate can inhibit the formation of substrate-directed parallel lamellae. When the air surface is sufficiently enthalpically neutral, the perpendicular lamellae can be observed. The structure of lamellar PS-PMMA diblock copolymer thin films on neutral poly(styrene-*random*-methyl methacrylate), P(S-*r*-MMA), brush surfaces was examined by Huang et al.^{22,23} Upon annealing, microphase separation occurs with perpendicular lamellae and parallel lamellae emanating from neutral substrate and air surface. Xu et al.²⁴ studied the surface effect on the structure of thin films with a lamellar morphology by using cross-section TEM; they found that the structure of thin films was determined by the difference in

* To whom correspondence should be addressed. Prof. Tianbai He: e-mail tbhe@ciac.jl.cn, Fax +86 431 85262126, Tel +86 431 85262123. Dr. Fajun Zhang: e-mail fajun.zhang@uni-tuebingen.de, Fax +49 7071 29 5110, Tel +49 7071 29 78670.

[†] Present address: National Creative Research Initiative Center for Block Copolymer Self-Assembly, Department of Chemical Engineering and Polymer Research Institute, Pohang University of Science and Technology, Kyungbuk 790-784, Korea.

interfacial energies between each component and the surface. If the difference in the interfacial energies was not strong enough, a mixed orientation of the lamellar domains could be observed.

In contrast with the condition where the substrate is neutral for both blocks in a symmetric diblock copolymer thin film, if two blocks have similar surface energy, then the polymer/air and polymer/polymer interface will be neutral for both blocks, too. Further, if one of the blocks shows strong affinity for the substrate, a reversed hybrid structure may be formed, i.e., parallel lamellae and perpendicular lamellae emanating from the substrate and neutral air surface. Recently, Olayo-Valles et al. reported that thin films of polystyrene–polylactide (PS–PLA) diblock copolymers form perpendicularly oriented cylinders and lamellae due to the similar surface energies of PS and PLA.^{25,26} However, little is known about the effect of interfaces during the structure formation in thin films. Moreover, the polymer/polymer interface is also a neutral interface for both blocks. What role does this interface play during an annealing procedure in thin films?

In this paper, we present the experimental results of a symmetric poly(styrene)-*b*-poly(L-lactide) (PS–PLLA) copolymer thin films on supported the silicon wafer surface. We focused our attention on the effects of both the initial film thickness and the annealing time on the lamellar orientation in thin films upon annealing. We found that the lamellar orientation of a film with film thickness larger than a lamellar period, L , was controlled by different interfaces in different stages during annealing. In early stage, the polymer/substrate interface dominates the lamellar orientation, resulting in a parallel lamellar orientation. The neutral polymer/polymer and polymer/air interfaces dominate the later stage of evolution, resulting in a transition of lamellar orientation from parallel to perpendicular with respect to the substrate. Some interesting intermediate structures are observed before reaching the equilibrium state.

Experimental Section

Materials. The diblock copolymer, PS–PLLA, was purchased from Polymer Source, Inc. The number-average molecular weight (M_n) is 40 500 (PS 21 000 and PLLA 19 500) with a polydispersity of 1.1 characterized by gel permeation chromatography (GPC). The total degree of polymerization is $N = 473$ determined by ^1H NMR. The volume fractions of PS and PLLA are 0.51 and 0.49, respectively. The temperature-dependent Flory–Huggins interaction parameter between PLA and PS reported by Zalusky et al.²⁸ was $\chi(T) = 98.1/T - 0.112$, where T is the Kelvin temperature and χ is the Flory–Huggins segmental interaction parameter. Assuming that the solubility parameters between PLA and PLLA are similar, the theoretical criterion of phase separation is $\chi(T_{\text{ODT}})N = 10.5$.^{1,29,30} The order–disorder transition temperature (T_{ODT}) of our system is calculated as $T_{\text{ODT}} = 458$ °C. The copolymer investigated here lies in strong segregation regime under present experimental conditions, i.e., $\chi N = 49$ and 47 at 180 and 190 °C, respectively. The long period of lamellar structure of PS–PLLA was $L = 25$ nm determined by SAXS.³¹ The surface energy of PLLA (38.3 mN/m)³² is similar to PS block (40.7 mN/m).³³

Thin Film Preparation. Polymer films were prepared by dissolving the sample in chloroform and spin-coating the solution onto freshly cleaned silicon wafer with native oxide layer. By controlling the concentration of polymer solution and spin speed, thin films with thickness ranging from 10 to 200 nm were obtained. All the wafers were cleaned in a mixture of H_2SO_4 , H_2O_2 , and H_2O (70/21/9 vol %) for 30 min at 120 °C, followed by extensive rinsing with deionized water. The cleaned wafers were dried in a stream of nitrogen and used immediately for the film deposition. The residual solvent was removed under vacuum for 24 h at room temperature. The film thickness was determined by ellipsometry

and AFM after scratching with a blade. Films with different thickness were annealed at 180 or 190 °C under vacuum for various times and then quenched to room temperature. The very similar FTIR spectra for thin films before and after annealing indicate that the copolymer does not degrade during sample preparation procedure (data not shown). The topography and structure of the resulting films were examined by AFM, TEM, and XPS.

Atomic Force Microscopy (AFM). Tapping mode AFM was conducted at ambient conditions using a SPA-300HV with a SPI3800N controller (Seiko Instruments Industry Co., Ltd., Japan). Both height and phase images were recorded simultaneously using the retrace signal. Etched Si tips with a resonance frequency of ~ 70 kHz and a spring constant of about 2 N/m were used, and the scan rate was in the range from 1.0 to 2.0 Hz. Each scan line contains 256 pixels, and a whole image is composed of 256 scan lines.

Transmission Electronic Microscopy (TEM). TEM experiments were performed on JEOL 1011 TEM with an accelerating voltage of 100 kV. The polymer thin films were floated from the silicon wafers and quickly transferred to copper grids. A saturated KOH solution at ~ 90 °C was used to etch away the silicon oxide layer and release the film. This method has been used to separate polymer thin films from substrate without altering the properties of the films.³⁴ To avoid damage, the samples were not stained, and the contrast came from the difference of the electron density between PLLA and PS (380 and 340 nm^{−3} for amorphous PLLA and PS, respectively.)

Field Emission Scanning Electronic Microscopy (FE-SEM). FE-SEM experiments were carried out on a Philips XL-30-ESEM-FEG. The samples were etched by UV for about 30 min and then rinsed in acetic acid for 15 min in order to remove the degraded PLLA. For cross-section observation, the sample was quenched and cut in liquid N_2 . Both the top and cross-sectional morphology were observed.³⁵

X-ray Photoelectron Spectroscopy (XPS). The surface chemical composition of thin films was determined with a VGESCALAB-MKII spectrometer with an Mg X-ray source. Pass energy of 20 eV was used to obtain the high resolution, and the takeoff angle of the X-ray source was 90°. The main chamber of the XPS instrument was maintained at 2.0×10^{-7} Pa during the spectral measurements. The relative photoelectron intensities of the C 1s peak (289 eV) were used to determine the composition of the upper layer of the polymer thin film.

Results and Discussion

1. Morphology and Structure of Thin Films: Initial Film Thickness Dependence. 1.1. Initial Film Thickness $h < L$. Figure 1 presents the results of thin films with an initial film thickness smaller than the lamellar repeat distance L . All the films presented in Figure 1 were annealed at 180 °C for 60 min under vacuum before quenching to room temperature. Further prolonging the annealing time gives the similar results (data not shown). Figure 1a presents the AFM height image of a thin film with $h \sim 10$ nm $< 1/2L$. The copolymer thin film dewets the substrate, forming droplets, indicating a disordered structure.^{36,37} Figure 1b shows the AFM height topography and the cross-section line profile for a thin film with $1/2L < h \sim 20$ nm $< L$. Holes with depth of about 25 nm are observed after annealing, in good agreement with symmetric wetting of PS–PLLA film over the oxidized silica surface.^{7–9} The TEM experiment (Figure 1c) further confirms the parallel orientation of the lamellae with respect to the substrate. Therefore, the top layer is PLLA due to the polar PLLA preferring to segregate to the substrate. Figure 1d shows the XPS profiles of relative photoelectron intensity of a film before and after annealing. The C 1s peak at 289 eV corresponds to the carbonyl group. The increase of the relative intensity of C 1s peak after annealing indicates that the top layer is mainly composed of PLLA.

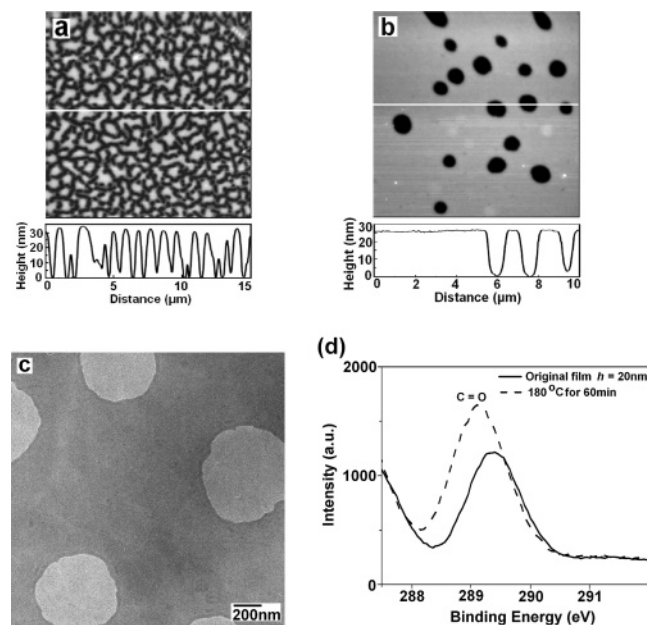


Figure 1. (a) AFM height topography and cross-section line profile of the thin film with $h \sim 10$ nm $< 1/2 L$ annealed at 180 °C for 60 min. The thin film with $1/2 L < h \sim 20$ nm $< L$ was annealed at 180 °C for 60 min. (b) AFM height topography and cross-section line profile. (c) TEM micrograph. (d) XPS C 1s spectra of $h \sim 20$ nm thin film before and after annealing at 180 °C for 60 min.

1.2. Initial Film Thickness $h > L$. Figure 2 shows the AFM and TEM results for samples with an initial film thickness larger than L . All the films presented in Figure 2 were annealed at 190 °C for 720 min under vacuum before quenching to room temperature. Figure 2a shows the AFM height topography and the cross-section line profile of a thin film with the thickness of $L < h \sim 33$ nm $< 3/2 L$. This is the situation discussed in our previous publication;³¹ we would further study the origin of this structure. We concluded that the symmetric wetting behavior of PLLA blocks results in a parallel lamellar structure with a continuous film having a thickness of L . The formation of islands on the free surface is due to the commensurability effect between h and L . However, the height of islands is about 32 nm, larger than the bulk repeat period $L = 25$ nm.³¹ Further investigations by TEM (Figure 2b) indicated that the lamellae within the islands are perpendicular to the substrate!

Increasing initial film thickness to $h \sim 42$ nm, $3/2 L < h < 2L$, as seen in Figure 2c,d, holes appear after annealing. However, the depth of holes is 32 ± 1 nm, larger than L but similar to the height of islands in the previous case (Figure 2a,b). The thickness of the bottom continuous film contact with the substrate is about 25 nm $= L$ (Figure 2c, the cross-section line profile). Figure 2d indicates that the top layer is composed of perpendicular lamellae, and the rim surrounding the hole is PLLA. The above observations reveal a hybrid lamellar structure for thin films of $h > L$; i.e., a perpendicular lamellar structure formed on the free surface while a parallel lamellar structure with thickness of L formed at the polymer/substrate interface.

Figure 2e shows the results of a thin film of $h \sim 55$ nm, $2L < h < 5/2 L$. One can still see the islands after annealing. The thickness of the continuous film measured by AFM after scratching the film is around 58 nm, which is the sum of a parallel lamella with thickness equals to L and a perpendicular lamellar layer with thickness of 33 nm. TEM micrograph (Figure 2f) indicates the perpendicular lamellae prevail in the whole free surface. Olayo-Valles et al. studied the domain orientation of thin films of a PS-PLA diblock copolymer with a lamellar

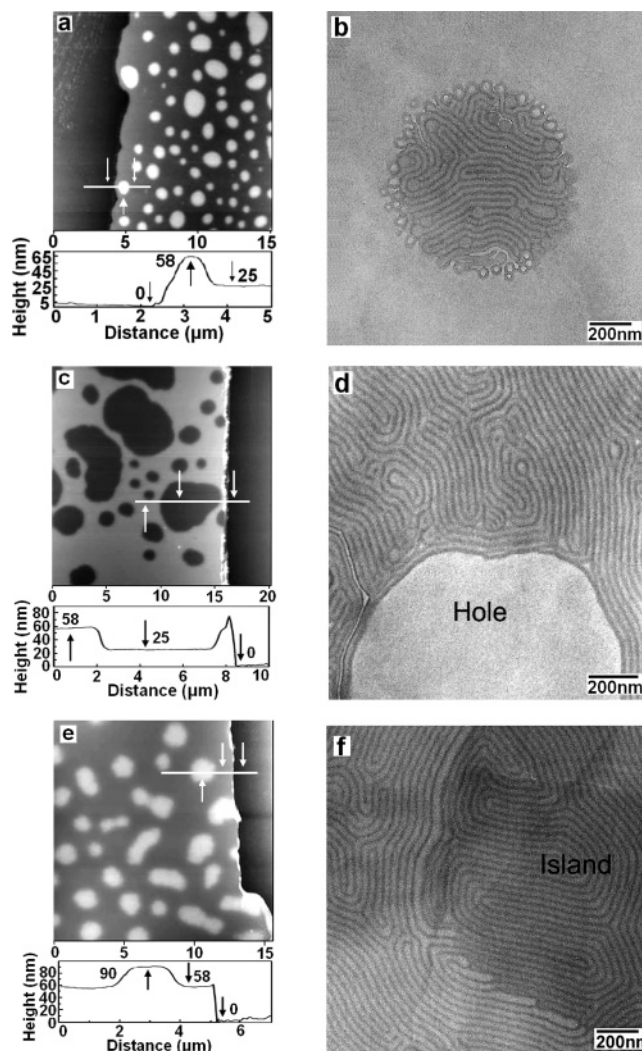


Figure 2. Thin films with different thickness were annealed at 190 °C for 720 min. (a) AFM height topography and cross-section profile of a thin film with $h \sim 33$ nm, $L < h < 3/2 L$. (b) Corresponding TEM micrograph of the thin film in (a). (c) AFM results of a thin film with $h \sim 42$ nm, $3/2 L < h < 2L$. (d) Corresponding TEM micrograph of the thin film in (c). (e) AFM results of a thin film with $h \sim 55$ nm, $2L < h < 5/2 L$. (f) Corresponding TEM micrograph of the thin film in (e).

morphology in bulk on the surface of a silicon wafer with a native oxide layer. For films of 70 nm, more than twice the lamellar period, $L = 32$ nm, they observed the perpendicular orientation of lamellar domain throughout the film. However, they did not report whether they could see the islands or not in their case. However, it is interesting to see that they observed the islands or holes in thin films of copolymers with a cylindrical morphology.^{25,26}

From Figure 1 and 2, a lamellar orientation transition could be seen from parallel to perpendicular with increasing the initial film thickness. The formation of the perpendicular lamellar structure at the polymer/air interface is due to the similar free energy of PS and PLLA. Theoretical and experimental studies have shown that the perpendicular orientation is favored for $h > L$ when there is negligible difference in the interfacial energies.³ An important consequence of forming perpendicular lamellae is flattening the whole film by reducing the holes or islands because the incommensurability effect of the initial film thickness can be accommodated by either increasing or decreasing the thickness of the perpendicular lamellar regions.^{21–24} Magerle et al.³⁸ have investigated the effect of surface fields on structure of cylinder-forming poly(styrene-*b*-butadiene-*b*-

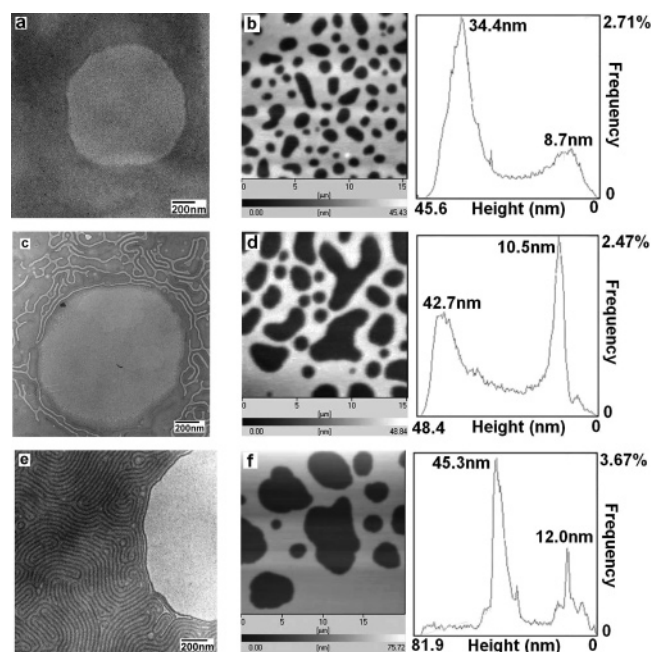


Figure 3. Morphologies of a thin film with $\frac{3}{2}L < h \sim 42 \text{ nm} < 2L$ annealed at 190°C for different time; TEM micrographs: (a) 5, (c) 240, and (e) 720 min. AFM height images and histogram analysis of the thin film annealed at 190°C for (b) 5, (d) 240, and (f) 720 min.

styrene) triblock copolymer thin films with different thickness. They concluded that the effect of surface fields could extend into the films with about one microdomain space. However, in our experiments, although the perpendicular lamellae formed on the top layer for $h > L$, one can still see the holes or islands up to $h \sim 6L$. Moreover, the thickness of the perpendicular regions (islands or the up layer with holes) is $\sim 33 \text{ nm}$ and almost does not change with film thickness. In order to explain these observations, the film structure and morphology during annealing are investigated and presented in the following sections.

2. Transition of Lamellar Orientation during Annealing.

2.1. Evolution of a Thin Film with $\frac{3}{2}L < h < 2L$. As a typical example, the results of a film with initial film thickness of 42 nm in the different annealing stages are presented in Figure 3. The final lamellar structure of this film as given in Figure 2c,d is a hybrid lamellar structure with a perpendicular lamellae layer with holes on above a parallel lamellae layer. The films were annealed at 190°C for a wide time period, ranging from 5 to 720 min, and the surface morphology was studied by TEM and AFM. In the very early annealing stage, i.e., annealing for 5 min (Figure 3a,b), holes appear on the free surface, and the contrast of the TEM micrograph is homogeneous throughout the film. The average depth of holes obtained from the histogram analysis (Figure 3b) is about 25.7 nm ($34.4 - 8.7 \text{ nm}$), in well agreement with the long period L in bulk. On the basis of these observations, it is obvious that a symmetric wetting structure (parallel lamellar) is formed throughout the film.⁷⁻⁹

With increasing the annealing time to 240 min, some perpendicular lamellae around holes appear (Figure 3c). It is interesting to see that the perpendicular lamellae form first at the edge of holes and spread to the interior of the films. Zhang et al. studied the boundary effect of holes and islands on crystallization of a symmetric PS-PCL diblock copolymer in thin films.^{39,40} They found nucleation events also prefer the edge of holes or islands, and they argued that the extended conformation of blocks in this region decreases the energy barrier for forming a critical nucleus. At the same time, the depth of holes

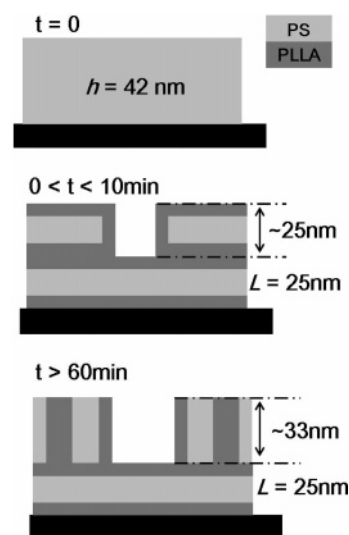


Figure 4. Schematic illustration of lamellar orientation transition during annealing in Figure 3.

increases to about 32.2 nm ($42.7 - 10.5 \text{ nm}$) determined from histogram analysis (Figure 3d). Further increasing the annealing time to 720 min (Figure 3e), the perpendicular lamellae fill the free surface except for the hole region. The depth of hole increases to about 33.3 nm ($45.3 - 12.0 \text{ nm}$) (Figure 3f). Further increasing the annealing times, the structure of thin film does not change with time.

The experimental results presented in Figure 3 clearly show that holes are formed in the early annealing stage and survived the further annealing. This means that the specific interaction between polymer and substrate dominates the lamellar orientation in the early annealing stage, resulting in a parallel lamellar structure. Holes are formed due to the incommensurability of the initial film thickness with the quantitative values (nL). Further prolonging the annealing time the neutral polymer/air interface starts to dominate the lamellar orientation. A transition from parallel to perpendicular orientation could be observed. During lamellar orientation transition, both the depth and the size of holes increase with time. Specially, the depth of holes in the early stage is close to the lamellar period L and increases step by step to a value around 33 nm . The reasons for this increase and why a value around 33 nm is stable in the final stage is not clear now. The parallel lamellae close to substrate do not change for further annealing. This transition process is illustrated in Figure 4. It is worth comparing our results with a system in which the substrate is a neutral interface while the air surface is a preferential interface. Huang et al.^{22,23} investigated the structure of lamellar poly(styrene-*b*-methyl methacrylate) diblock copolymer films on neutral poly(styrene-*r*-methyl methacrylate) brush surfaces as a function of annealing time and film thickness. They found that upon annealing microphase separation occurred simultaneously with perpendicular and parallel lamellae emanating from the neutral and air surfaces, respectively.^{22,23} While in our case the two interfaces play a dominant role in different annealing stages, the preferential polymer/substrate interface dominates in the early stage, while the neutral air surface dominates in the subsequent stage accompanying a lamellar orientation transition.

2.2. Evolution of a Thin Film with $h > 2L$. As mentioned above, the polymer/polymer interface is also a neutral interface for both blocks due to the similar free energies. In order to see the role of this interface during the evolution of lamellar orientation in thin films, a thin film with $h \sim 55 \text{ nm}$ in different

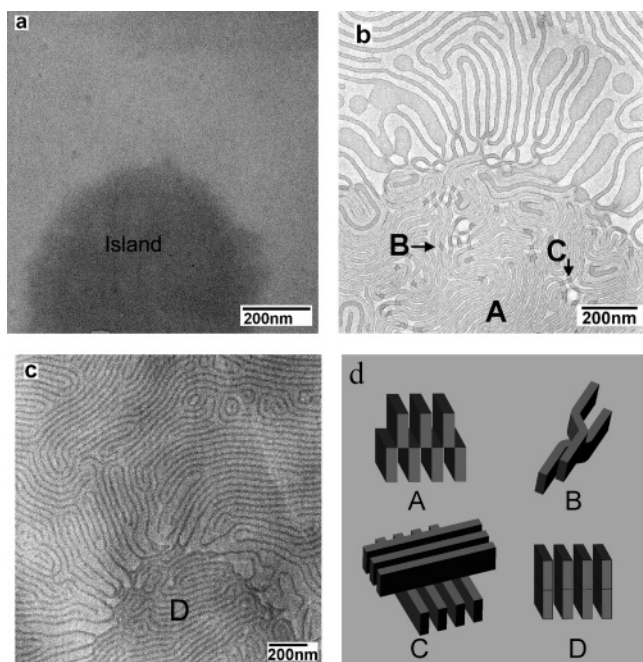


Figure 5. TEM micrographs of the thin film with $2L < h \sim 55 \text{ nm} < 5/2L$ annealed at 190°C for (a) 5, (b) 240, and (c) 720 min. (d) Schematic illustration of interlayer defects labeled in (b) and (c).

annealing stages has been studied. Figure 5a is the TEM micrograph of a thin film annealed at 190°C for 5 min. Again, islands appear on the surface and the contrast is homogeneous, indicating the formation of a parallel lamellar structure. Increasing annealing time to 360 min (Figure 5b), perpendicular lamellae form not only in the islands but also in the continuous film around the islands. Surprisingly, the perpendicular lamellae within the islands and the continuous film are different. The perpendicular lamellae are interlaced in the island forming various defects as shown in Figure 5d. These defects are formed due to the overlapping of two layers; each has a perpendicular lamellar structure with random lamellar orientation. As indicated in the Introduction, the polymer/polymer interface in PS-PLLA block copolymer is a neutral interface for both blocks; therefore, the lamellar orientation transition could occur within the parallel lamellar domains with polymer/air and polymer/polymer interfaces. Further increasing annealing time to 720 min, the perfect uniform perpendicular lamellae are formed in the surface of thin film (Figure 5c). Figure 5d illustrates the typical defects (A, B, C) and the final stable stage (D) formed by perpendicular lamellae in two adjacent parallel layers as labeled in Figure 5b,c.

The results shown in Figure 5 clearly display the role of polymer/polymer interface during the lamellar orientation transition and the formation of the defects, as illustrated in Figure 6. In the early stage, the effect of substrate leads to the formation of three lamellae layers with parallel orientation; the thickness of each lamella is $1L$, i.e., the first full layer directly in contact with substrate, the second full layer on above the first layer, and the third top layer formed by islands. Further annealing, the lamellar orientation transition starts in the top two layers except the layer attached by the substrate. The interesting observation is that the lamellar orientation transition occurs in these two layers independent of each other; i.e., the perpendicular lamellae formed in islands and the layer beneath the islands are randomly oriented in the flat 2D plane, which results in the interlaced lamellar structure, as illustrated in Figure 5d. Such structures are definitely not the thermodynamic stable form. Upon further annealing, the defects between layers emerge gradually, resulting in uniform perpendicular lamellae.

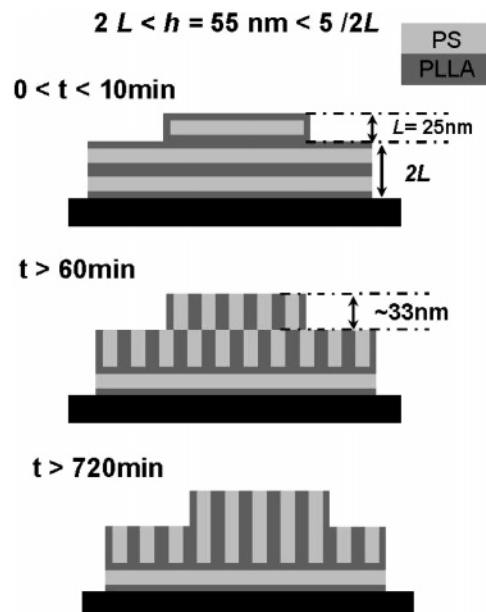


Figure 6. Schematic illustration of lamellar orientation transition in different layers during annealing, as shown in Figure 5.

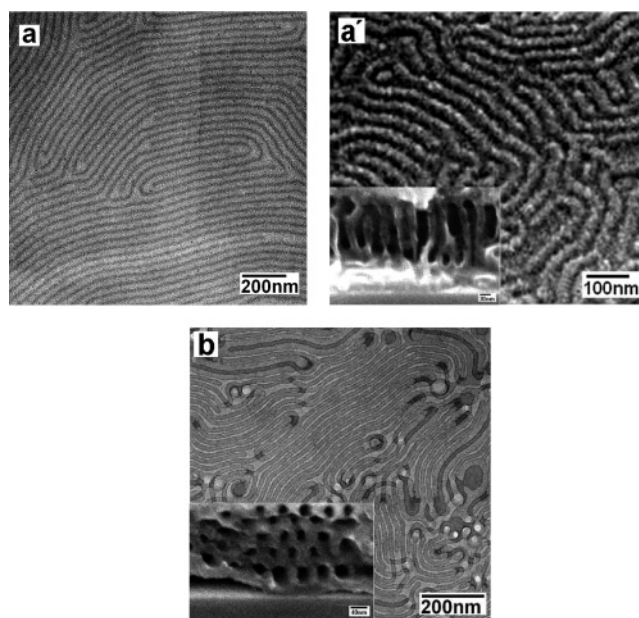


Figure 7. Micrographs of the thin film ($h \sim 150 \text{ nm} = 6L$) annealed at 190°C for (a) 720 min, TEM micrograph; (a') 720 min, SEM micrograph; and (b) 360 min, TEM micrograph. The insets in (a') and (b) are cross-sectional images obtained by FE-SEM; all PLLA phases were etched using UV.

2.3. Evolution of a Thin Film with $h \geq 6L$. The lamellar structure and orientation competition observed in previous sections (2.1 and 2.2) can persist up to a film thickness of $6L$. Above this thickness, islands or holes disappear in thin films. The morphology and structure of such thin films can be described by using the surface TEM micrograph and cross-sectional SEM micrograph. Figure 7a displays a TEM micrograph of a thin film of 150 nm equal to $6L$ annealed at 190°C for 720 min. Perfect perpendicular lamellae were observed throughout the film. The dark regions are PLLA and the bright regions are PS. Figure 7a' is the corresponding SEM top-view micrograph, and the inset is the corresponding SEM cross-sectional micrograph. The bright regions are PS, and the dark regions are PLLA. The cross-sectional micrograph demonstrates that the lamellae are oriented perpendicular to the surface. The

volumes of PLLA to PS are similar to each other within the error in TEM and SEM micrographs. To investigate the structure evolution of these thicker films in the early stage, thin films were annealed for a shorter time before observation. Figure 7b shows TEM micrograph of a film annealed at 190 °C for 360 min; morphology and structure of the thin film are similar to the island shown in Figure 5b. Various defect patterns could be observed (illustrated in Figure 5d). The inset in Figure 7b shows the corresponding SEM cross-sectional micrograph, which exhibits that one parallel layer attached to the substrate and above it; perpendicular lamellae are formed independently in each layer. Therefore, their parallel, mismatch, or interlace to each other result in the defect patterns observed on the top-view of the thin film. Because of geometric confinement, it is possible that the cylinder microdomains are in the intermediate state. Further decreasing the annealing time, the structure of thin film is similar to Figure 7b. Even if in the initial annealing stage, complete parallel lamellae or islands or holes cannot be observed anymore because the film is so thick that the polymer/air interface dominates the evolution of the film structure.⁴¹

It is worth to note that our observations on the formation of an intermediate stage during the structure evolution in symmetric block copolymer thin films can be generalized to antisymmetric block copolymer thin films and rod-coil copolymer thin films.^{25,26,41} For example, in thin films of a diblock copolymer with a cylindrical morphology in bulk, the commensurate effect can also result in the formation of islands or holes on the free surface when the cylinder domains are parallel to the substrate. Olayo-Valles et al.^{25,26} observed the formation of islands or holes in thin films of a PS-PLA diblock copolymer when the initial film thickness below the center-to-center distance between closest-neighbor cylinders. Moreover, a mixed orientation of parallel and perpendicular cylinder domain was observed. For thicker films, on the other hand, smooth surfaces with predominately perpendicular cylinder domains were observed. On the basis of our observations in sections 1 and 2, we believe that an intermediate stage with fully parallel orientation of cylinder domains may exist in the early stage of annealing, which account for the formation of islands or holes for the thinner films.

We also note that the morphologies reported in this work are not observed in the well-documented PS-PMMA system in which the surface energies of the two blocks are very similar to each other. We noticed that in our system PLLA has a lower surface energy (38.3 mN/m) than that of PS (40.7 mN/m).³³ While for PS-PMMA, however, although the surface energy of PMMA (41.1 mN/m)⁴² is very close to PS, it is actually higher than that of PS. This may be the main reason for the absence of the morphologies observed in this work.

Conclusions

We have studied the domain orientation of symmetric PS-PLLA diblock copolymer thin films in melt state. For thin films with the initial film thickness $\frac{1}{2}L < h < L$, a symmetric wetting structure with parallel lamellae is formed. Increasing the initial film thickness larger than the bulk repeat period, i.e., $L < h$, a hybrid structure is formed. Holes or islands formed due to the commensurability effect could be observed up to $h \sim 6L$ and then disappear with further increasing film thickness. A transition of lamellar orientation was observed in thin films with different thickness ($\frac{3}{2}L < h < 6L$) during annealing. In our system, the surface energies of PS and PLLA are similar to each other, which results that the polymer/air and polymer/polymer interfaces are neutral for both blocks, while the PLLA

block prefers to absorb on the substrate due to the polar interaction. Both effects on the initial film thickness and annealing time were investigated. In the early annealing stage the specific interaction between polymer and substrate dominates the lamellar orientation, resulting in a parallel lamellar structure. Further prolonging the annealing time, the neutral polymer/air and polymer/polymer interfaces start to dominate the lamellar orientation and lead to the perpendicular lamellar structure. Because of the neutrality of polymer/polymer interface, for films with thickness $h > 2L$, the lamellar orientation transition can occur independently in different parallel lamellar domains. This independent transition leads to a new intermediate stage; i.e., the perpendicular lamellae in two adjacent layers can be either parallel or cross to each other. Certainly, these interlaced structures are not the thermodynamic equilibrium forms. They emerge into the uniformed perpendicular structure upon further annealing. The origin and structure transition of thin film are different from those of perpendicular lamellae induced by crystallization.³¹

Acknowledgment. The authors thank Dr. Bingyang Du (Zhejiang University, China) for helpful discussion and constructive suggestions. This work is supported by National Science Foundation of China (20574068) and the Chinese Academy of Sciences (KJCX2-SW-H07) and subsidized by National Basic Research Program of China (2005CB6238).

References and Notes

- Hamley, I. W. *The Physics of Block Copolymers*; Oxford University Press: New York, 1998.
- Green, P. F.; Limary, R. *Adv. Colloid Interface Sci.* **2001**, *94*, 53.
- Fasolka, M. J.; Mayers, A. M. *Annu. Rev. Mater. Res.* **2001**, *31*, 323.
- Morkved, T. L.; Lu, M.; Urbas, A. M.; Ehrichs, E. E.; Jeager, H. M.; Mansky, P.; Russell, T. P. *Science* **1996**, *273*, 931.
- Thurn-Albrecht, T.; Schotter, J.; Kaestle, G. A.; Emley, N.; Shibauchi, T.; Krusin-Elbaum, L.; Guarini, K.; Black, C. T.; Tuominen, M. T.; Russell, T. P. *Science* **2000**, *290*, 2126.
- Park, C.; Yoon, J.; Thomas, E. L. *Polymer* **2003**, *44*, 6725.
- (a) Russell, T. P.; Coulon, G.; Deline, V. R.; Miller, D. C. *Macromolecules* **1989**, *22*, 4600. (b) Bassereau, P.; Brodbreck, D.; Russell, T. P.; Brown, H. R.; Shull, K. R. *Phys. Rev. Lett.* **1993**, *70*, 1716. (c) Anastasiadis, S. H.; Russell, T. P.; Satija, S. K.; Majkrzak, C. F. *Phys. Rev. Lett.* **1989**, *62*, 1852. (d) Mayes, A. M.; Russell, T. P.; Bassereau, P.; Baker, S. M.; Smith, G. S. *Macromolecules* **1994**, *27*, 749. (e) Cai, Z.; Huang, K.; Montano, P. A.; Russell, T. P.; Bai, J. M.; Zajac, G. W. *J. Chem. Phys.* **1993**, *98*, 2376.
- Grim, P. C. M.; Nyrkova, I. A.; Semenov, A. N.; ten Brinke, G.; Hadzioannou, G. *Macromolecules* **1995**, *28*, 7501.
- Sohn, B. H.; Seo, B. W.; Yoo, B. I.; Zin, W. C. *Z. Langmuir* **2002**, *18*, 10505.
- Maaloum, M.; Ausserre, D.; Chatenay, D.; Gallot, Y. *Phys. Rev. Lett.* **1993**, *70*, 2577.
- Sikka, M.; Singh, N.; Karim, A.; Bates, F. S.; Satija, S. K.; Majkrzak, C. F. *Phys. Rev. Lett.* **1993**, *70*, 307.
- (a) Coulon, G.; Daillant, J.; Collin, B.; Benattar, J. J.; Gallot, Y. *Macromolecules* **1993**, *26*, 1582. (b) Coulon, G.; Russell, T. P.; Deline, V. R.; Green, P. F. *Macromolecules* **1989**, *22*, 2581.
- Pickett, G. T.; Witten, T. A.; Nagel, S. R. *Macromolecules* **1993**, *26*, 3194.
- Pereira, G. G.; Williams, D. R. M. *Macromolecules* **1999**, *32*, 1661.
- Potemkin, I. I. *Macromolecules* **2004**, *37*, 3505.
- Kellogg, G. J.; Walton, D. G.; Mayes, A. M.; Lambooy, P.; Russell, T. P. *Phys. Rev. Lett.* **1996**, *76*, 2503.
- Stocker, W. *Macromolecules* **1998**, *31*, 5536.
- Peters, R. D.; Yang, X. M.; Nealey, P. F. *Macromolecules* **2002**, *35*, 1822.
- Busch, P.; Posselt, D.; Smilgies, D.-M.; Rheinländer, B.; Kremer, F.; Papdakis, C. M. *Macromolecules* **2003**, *36*, 8717.
- Sivaniah, E.; Hayashi, Y.; Iino, M.; Hashimoto, T. *Macromolecules* **2003**, *36*, 5894.
- Sivaniah, E.; Hayashi, Y.; Matsubara, S.; Hashimoto, T. *Macromolecules* **2005**, *38*, 1837.
- Huang, E.; Harrison, C.; Russell, T. P. *Macromolecules* **1998**, *31*, 7641.
- Huang, E.; Mansky, P.; Russell, T. P. *Macromolecules* **2000**, *33*, 80.
- Xu, T.; Hawker, C. J.; Russell, T. P. *Macromolecules* **2005**, *38*, 2802.

- (25) Olayo-Valles, R.; Guo, S.; Lund, M. S.; Leighton, C.; Hillmyer, M. A. *Macromolecules* **2005**, *38*, 10101.
- (26) Olayo-Valles, R.; Lund, M. S.; Leighton, C.; Hillmyer, M. A. *J. Mater. Chem.* **2004**, *14*, 2729.
- (27) In, I.; La, Y.-H.; Park, S.-M.; Nealey, P. F. *Langmuir* **2006**, *22*, 7855.
- (28) Zalusky, A. S.; Olayo-Valles, R.; Wolf, J. H.; Hillmyer, M. A. *J. Am. Chem. Soc.* **2002**, *124*, 12761.
- (29) Bates, F. S.; Fredrickson, G. H. *Annu. Rev. Phys. Chem.* **1990**, *41*, 525.
- (30) Leibler, L. *Macromolecules* **1980**, *13*, 1602.
- (31) Chen, D.; Gong, Y.; He, T.; Zhang, F. *Macromolecules* **2006**, *39*, 4101.
- (32) (a) Murphy, W. L.; Mooney, D. J. *J. Am. Chem. Soc.* **2002**, *124*, 1910. (b) Irvine, D. J.; Ruzette, A. V. G.; Mayes, A. M.; Griffith, L. G. *Biomacromolecules* **2001**, *2*, 545.
- (33) Green, P. F.; Thomas, M.; Christensen, T. M.; Russell, T. P. *Macromolecules* **1989**, *22*, 2189.
- (34) (a) Liu, Y.; Zhao, W.; Zheng, X.; Rafailovich, M. H.; Sokolov, J. *Macromolecules* **1994**, *27*, 4000. (b) Liu, Y.; Rafailovich, M. H.; Sokolov, J. *Macromolecules* **1996**, *29*, 899.
- (35) (a) Jeong, U.; Ryu, D. Y.; Kho, D. Y.; Kim, J. K.; Russell, T. P. *Adv. Mater.* **2004**, *16*, 533. (b) Park, M. S.; Lee, Y.; Kim, J. K. *Chem. Mater.* **2005**, *17*, 3944.
- (36) Liu, Y.; Loo, Y.-L.; Register, R. A.; Green, P. F. *Macromolecules* **2005**, *38*, 7745.
- (37) Green, P. F.; Limary, R. *Macromolecules* **1999**, *32*, 8167.
- (38) Knoll, A.; Horvat, A.; Lyakhova, K. S.; Krausch, G.; Sevink, G. J. A.; Magerle, R. *Phys. Rev. Lett.* **2002**, *89*, 035501.
- (39) Zhang, F.; Chen, Y.; Huang, H.; Hu, Z.; He, T. *Langmuir* **2003**, *19*, 5563.
- (40) Zhang, F.; Huang, H.; Hu, Z.; Chen, Y.; He, T. *Langmuir* **2003**, *19*, 10100.
- (41) Olsen, B. D.; Li, X.; Wang, J.; Segalman, R. A. *Macromolecules* **2007**, *40*, 3287.
- (42) Brandrup, J.; Immergut, E. H., Eds.; *Polymer Handbook*, 3rd ed.; John Wiley & Sons: New York, 1989.

MA070922N